SHRP-C-627

Development of Transient Permeability Theory and Apparatus for Measurements of Cementitious Materials

D.M. Roy
B.E. Scheetz
J. Pommersheim
P.H. Licasttro

Materials Research Laboratory
The Pennsylvania State University
University Park, Pennsylvania

Strategic Highway Research Program
National Research Council
Washington, DC 1993

SHRP–C–627
Contract C-201

Program Manager: *Don M. Harriott*
Project Manager: *Inam Jawed*
Production Editor: *Marsha Barrett*
Program Area Secretary: *Ann Saccomano*

April 1993

key words:
equipment design
fluid flow
model development
permeability
pressure decay
pressure differential
transient pressure pulse

Strategic Highway Research Program
National Academy of Sciences
2101 Constitution Avenue N.W.
Washington, DC 20418

(202) 334-3774

350/NAP/493

Acknowledgments

The research described herein was supported by the Strategic Highway Research Program (SHRP). SHRP is a unit of the National Research Council that was authorized by section 128 of the Surface Transportation and Uniform Relocation Assistance Act of 1987.

Contents

Abstract

A permeability apparatus was designed and constructed that would allow a rapid and accurate measurement of water transport in concrete. The principle of the apparatus was to subject a test specimen to a small pressure differential and to monitor both the pressure decay and the pressure rise resulting in response to the pressure pulse. The apparatus consists of a design which can isolate two pressurized, large volume reservoirs on both sides of the test specimen where the test specimen was acting as a permeable membrane between the two. Very rapid measurements are possible with this apparatus for specimens possessing permeabilities on the order of microdarcy to nanodarcy. However, in order to measure permeabilities below a nanodarcy the problems of establishing pressure equilibration throughout the test specimen becomes increasingly more difficult.

To explain the behavior of cementitious materials subjected to pressure, mathematical relationships were developed building upon the work in existing literature on fluid flow in porous media subjected to a transient pressure pulse.

EXECUTIVE SUMMARY

The durability of concrete is frequently associated with the transport of dissolved species. Such transport may be considered in terms of permeability. It is well recognized that transport occurs through a continuous network of pores, which exist in the cementitious matrix of concrete, as well as through the porosity which exists in the interfacial regions of aggregate. It is the objective of this report to describe work leading to rapid and accurate measurement of concrete permeability and the development of the theory to describe permeability of concrete.

A transient pressure permeability apparatus was designed and constructed that would allow a rapid and accurate measurement of water transport in concrete. The apparatus consists of a design which can be closed in a manner to isolate pressurized large volume reservoirs with the test specimen acting as a permeable membrane between the two. A differential pressure is established and both the pressure decay and the pressure rise are monitored. Very rapid measurements are possible with this apparatus of specimens possessing permeabilities of the order of microdarcy to nanodarcy. However, in order to measure permeabilities below a nanodarcy the problems of establishing pressure equilibration throughout the test specimen becomes increasingly more difficult.

In conjunction with the apparatus of construction, the detailed mathematical relationships building upon the original work of Brace et al. (1981), Lin (1977) and Hsieh et al. (1971) were also developed.

DEVELOPMENT OF TRANSIENT PERMEABILITY THEORY AND APPARATUS FOR MEASUREMENTS OF CEMENTITIOUS MATERIALS

INTRODUCTION

The assumption that the permeability of concrete is a physical property measurement which can be used as an indicator of the quality of concrete has not changed since the outset of this research program. Mortar samples prepared in this laboratory routinely achieve a permeability to water of <10 nanodarcy which is equivalent to the values of 10^{-16} cm^2 for quality concrete such as those reported by Hooton (1988) and other workers.

The measurement of very low values of permeability presents special problems for which standard measuring techniques are generally impractical or very difficult to implement and therefore tend to be unreliable (Roy, 1988). If the permeability is very low, long periods of time are required to establish steady state flow conditions which are for the most part impractical. To overcome these limitations, Brace et al. (1968) introduced a transient flow method to measure permeability of Westerly granite to water. In this experimental design, cylindrical specimens of the granite were contained in a flexible sleeve and connected to an up-stream and down-stream fluid reservoir. At the start of the experiment, both reservoirs and the specimen were maintained at the same constant pressure. Fluid flow was initiated through the specimen by rapidly establishing a pressure gradient between the up-stream and down-stream reservoirs. As the pressure began to decay through the sample, it was monitored and from this pressure decay, the permeability was calculated.

Introduction to Theory of Pressure Pulse Testing

Transient decays in pressure have been used in the pressure-pulse permeability cell* to successfully measure hydraulic properties of materials of low permeability such as cored samples of rocks and sandstones (Brace et al. , 1968; Hsieh et al., 1981; Neuzil et al., 1981). To date, there has been little work devoted to the application of this technique to cementitious materials, which generally have higher compressibilities and permeabilities (Hooton and Wakeley, 1989). In the transient pressure pulse method described below, the jacketed sample is confined between two pressurized reservoirs which contain the penetrating fluid. The pores of the sample are also filled with the fluid. The jacket or confining pressure is kept higher than the reservoir pressures. When the experiment begins, the pressure in one of the reservoirs is suddenly changed to a higher or lower value and the resultant pressure changes on the high or low pressure side are measured as a function of time.

One of the best ways of collecting data is to simultaneously measure the pressure change in both reservoirs. However, few researchers have used this method. Pommersheim and Scheetz (1989) have recently discussed the advantages of this technique. Hooton and Wakeley (1989) have emphasized the sensitivity of test results to environmental variables when measurement water permeabilities of concrete.

As part of a larger study made to characterize the microstructure and transport properties of concrete, we have conducted experiments with cylindrical cores of cements and mortars using both the pressure pulse cell and flow-through cells in order to determine and compare their permeabilities. Further experimental details can be found in Part II of this report along with the application of the theory developed in this part to the determination of sample permeabilities from data collected in pressure pulse tests.

---

* Also known as the triaxial or Hassler cell.

Figure 1 presents a schematic diagram showing the experimental configuration for the transient pressure pulse test. Before the test begins the entire system is at a constant pressure P_o. Then the pressure in the upstream reservoir (P_u) is suddenly increased to P_1, while the downstream reservoir (P_d) remains at P_o. P_u will fall and P_d will rise as fluid is transferred between the reservoirs. A constant confining pressure (P_c) is kept outside the sample. By maintaining this pressure at a level considerably higher than P_1, leaks are prevented. However P_c cannot be kept too high because of the possibility of creep or micro-cracking or decreasing the permeability of the sample by closing otherwise open porosity.

Figure 2 is a schematic representation showing how the upstream and downstream pressures change with time for a material which typically has low permeability and compressibilities. The figure illustrates the case where the two reservoir volumes, V_u and V_d, are equal. Nomenclature is provided beneath the figure. The curves are the pressure decay and pressure rise curves for the granite. Here the response of the two curves is symmetric around a horizontal line drawn to the final pressure P_f reached by both reservoirs. As discussed by Pommersheim and Scheetz (1989), the analysis of Brace et al. (1968) predicts that this pressure will lie midway between P_0 and P_1, while the analysis of Hsieh et al. (1981) predicts that P_f will lie more towards the upstream side. The difference is attributable to the fact that Brace and coworkers assumed in their development that the compressive storage of the sample was negligible, whereas Hsieh and coworkers did not. P_f can also be estimated from a mass balance knowing the pore volume of the sample and the volumes and initial pressures in the reservoirs (Trimmer, 1981).

Figure 3 illustrates typical transient pressure responses for cementitious materials, which usually have relatively high porosities, compressibilities, and permeabilities. The pressure changes observed are more rapid for such materials and are not symmetric with one another. In this instance, it is observed that the final pressure is no longer equal to the average of the initial pressures but is skewed towards the high pressure side of the pulsed reservoir. The rapid changes in pressure observed at early times appear to indicate that the sample is more compressible at higher pressures.

In order to explain such apparently anomalous behavior it is necessary to first develop and solve a mathematical model which predicts how the pressure changes within the sample and the reservoirs. The theory for this process is developed in this section and then applied in the next, where general procedures are presented for determining permeabilities of cementitious materials from experimental data.

Model Development

Previous mathematical models for pressure pulse testing have been developed by Brace et al. (1968), Lin (1977), Hsieh et al. (1981) and Pommersheim and Scheetz (1989).

As a model system consider the cylindrical sample depicted in Figure 1 presented earlier, having total volume V = AL, where A is the cross-sectional area of the specimen and L its length. The sample is confined between two pressurized reservoirs, the upstream one at P_u and the downstream one at P_d. The initial values of the upstream and downstream pressures are P_1 and P_0, respectively.

The partial differential equation which governs pressure changes as a function of distance and time P(x,t) within the sample is given by:

$$\frac{\partial^2 P}{\partial x^2} + \beta'\left(\frac{\partial P}{\partial x}\right)^2 = \frac{\beta u}{k}\frac{\partial P}{\partial t} \qquad (1)$$

SCHEMATIC DRAWING OF PERMEABILITY APPARATUS DESIGN

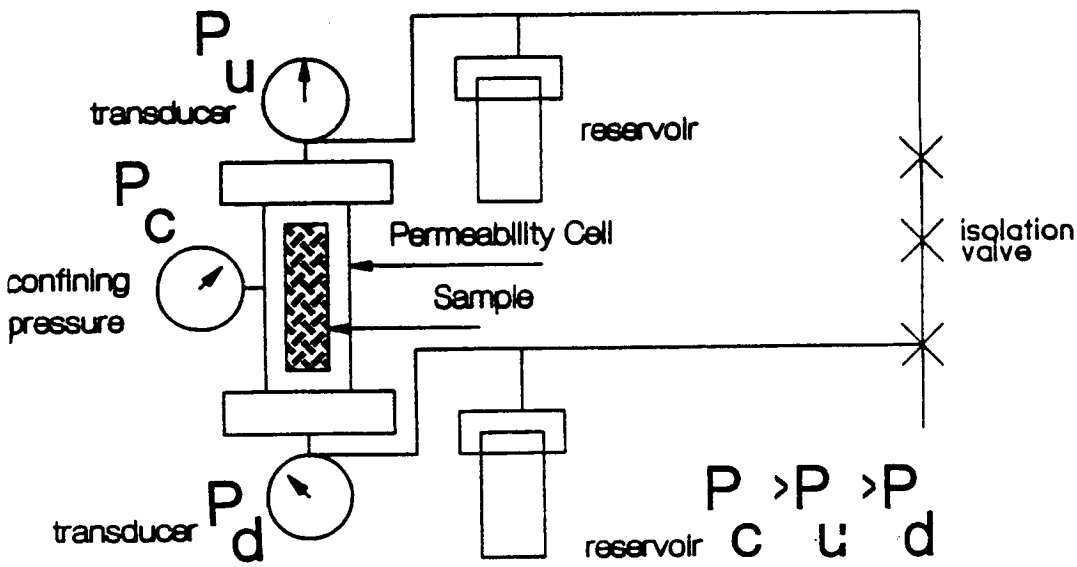

Figure 1. Schematic drawing of permeability apparatus.

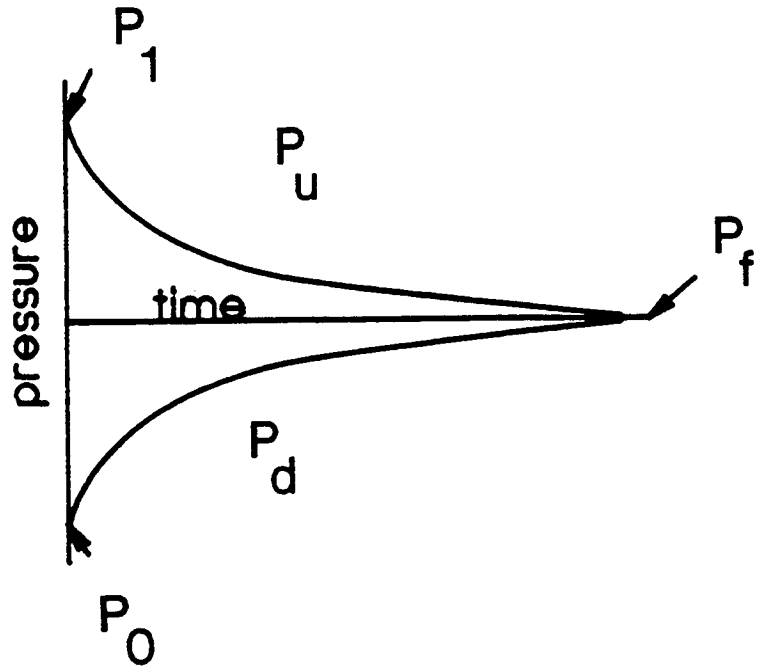

P_u = up-stream pressure
P_d = down-stream pressure
P_f = final equilibrated pressure [~$(P_1 + P_0)/2$]
P_1 = initial up-stream pressure
P_0 = initial down-stream pressure

Figure 2. Schematic representation of up-stream and down-stream pressure response as a function of time during the experiment.

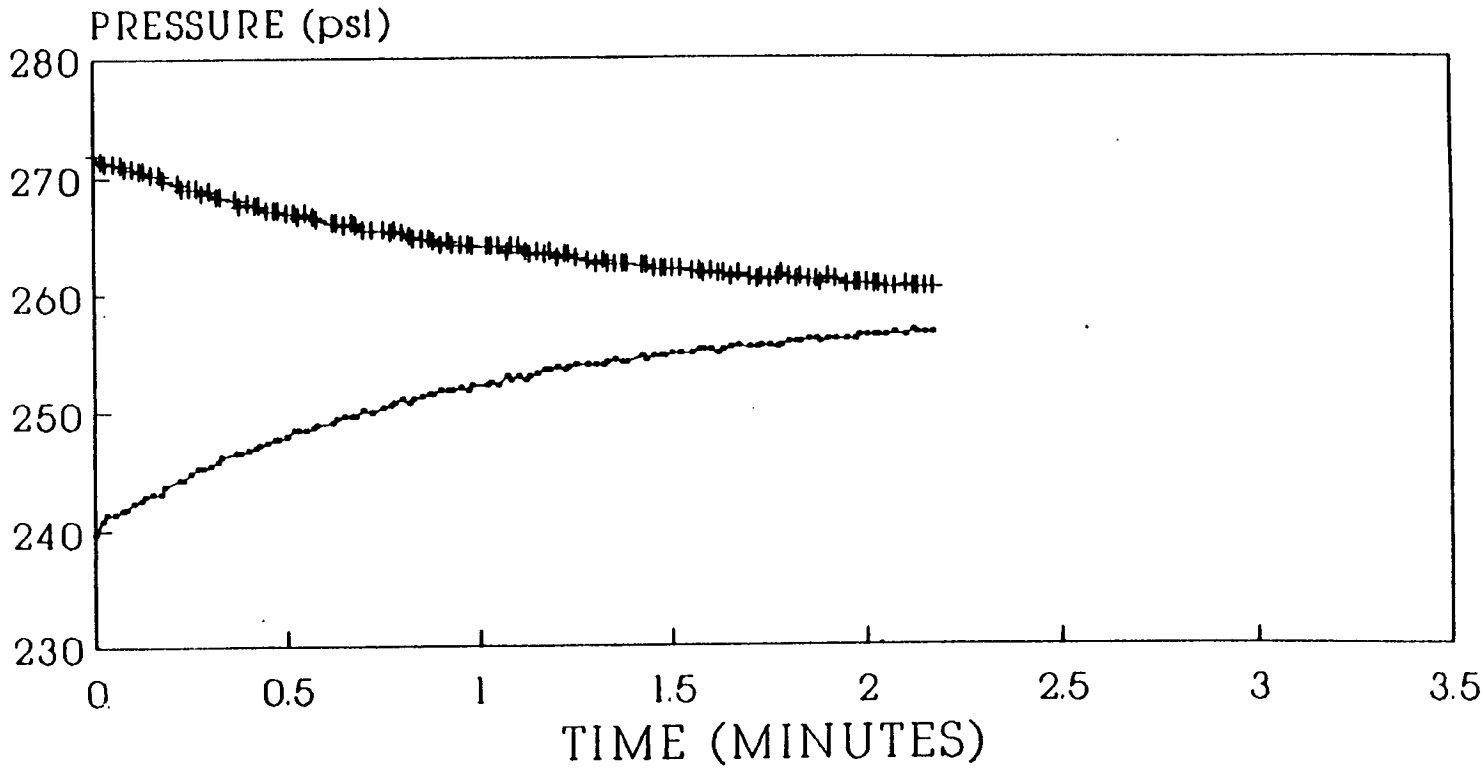

Figure 3. Typical raw data for mortar that has cured for one day. Permeability is approximately 10 microdarcy.

where P = pressure within the sample;
μ = pore fluid viscosity;
k = sample permeability;
x = axial distance within the sample, measured from the upstream reservoir;
t = time;
β' = lumped compressibility.

The derivation of Equation (1) is presented in Appendix 1. Equation (1) represents how the pressure P(x,t) varies within the sample as a function of position x and time t. It is a nonlinear partial differential equation subject to one time and two boundary conditions. These are given by:

$P(x,0) = P_o$ initial condition

$P(0,t) = P_u(t)$ boundary conditions

$P(L,t) = P_d(t)$

where L = sample thickness;
P_u, P_d = upstream and downstream pressures, respectively.

Assumptions involved in the derivation of Equation (1) include: one dimensional mass transfer with constant transport area, constant temperature, and constant physical properties (μ, k, β' and porosity). These assumptions are the same as those stated or implied by previous workers (Brace et al., 1968, Hsieh et al., 1981). Most of them are likely to be met in laboratory tests with homogeneous corings. Sample compressibilities will be most likely to remain constant when the ratio of the confining pressure to the initial pressure different, i.e., $P_c/(P_1-P_0)$ is high (Wooton and Wakeley, 1989).

β' is a lumped compressibility. It depends on the compressibility of the fluid, β, the compressibility of the sample, β_s, the effective compressibility of the jacketed sample, β_e, and the sample porosity, ε, according to:

$$\beta' = (\beta_e - \beta_s) + \varepsilon(\beta - \beta_e) \tag{2}$$

A similar equation has been presented by Brace et al. (1968) and by Hsieh et al. (1981). Of all these quantities β_e is the one which is least likely to be known and which is also potentially the largest, especially in experimental configurations where the sample is retained in a flexible rubber or plastic sleeve. In effect this makes β_e, and thus β', an arbitrary parameter. Neuzil et al. (1981) found values for this parameter which were several orders of magnitude greater than the fluid compressibility.

By introducing the dimensionless distance $z = x/L$, the $\theta = t/T$, and pressure $P = (P-P_0)/\Delta P$, Equation (1) and its attendant conditions become:

$$\frac{\partial^2 p}{\partial z^2} + \beta'\Delta P \left(\frac{\partial p}{\partial z}\right)^2 = \frac{\partial p}{\partial \theta} \tag{3}$$

(I) (II) (III)

where $\Delta P = P_1 - P_0$.

with conditions: $p(0,\theta) = p_u(\theta)$ reduced boundary conditions
$p(1,\theta) = p_d(\theta)$
$p(z,0) = 0$ reduced initial condition

$T = \beta'\mu L^2/k$ is a characteristic time for the transfer of mass from the high pressure to the low pressure side.

The terms in Equation (3) have been labeled (I), (II) and (III). Term (I) represents the transfer of mass between reservoirs caused by the pressure difference. It is present in all formulations of the problem. The unsteady state term (III) corresponds to the accumulation of mass within the sample. If the observed experimental times t are much greater than the characteristic time T, i.e. $t >> T$, then the accumulation term can be neglected. This is a requirement of a steady state process. However, since the pressures at the two ends of the sample are continuously changing, pressures within the system slowly adjust to accommodate these changes, in effect adjusting to each new steady-state. Such behavior is called quasi-static and the system is said to be at quasi-steady state.

Term (II) in Equation (3) represents the dynamic response to the compression of the jacketed sample. This non-linear term will be small when the dimensionless compressibility $\beta'\Delta P$ is small. Calculations show that term (II) would be small if β' is of comparable magnitude to the compressibility of the fluid, but, as discussed, this is often not the case in practice.

Table 1 summarizes the mathematical solutions different workers have found in Equation (1) and its variants. In the solutions of Brace et al. (1968) and Pommersheim and Scheetz (1989), only term (I) was retained. This predicts a linear pressure profile across the sample. The solution of Hsieh et al. (1981) is the only one which allows directly for transient pressure changes within the sample. The others must rely on a quasi-steady state analysis in order to predict transient pressures within the reservoirs. However the treatment of Hsieh et al. (1981) did not consider the non-linear term (II). Their analytical solution was obtained by Laplace transform methods. It took the form of an infinite series and involved three dimensionless parameters: a dimensionless time and two dimensionless compressive storage or compressibility ratios.

To complete the formulation it is necessary to obtain conservation equations for the upstream and downstream reservoirs. These are shown as Equations (4) and (5), respectively:

$$-\frac{dP_u}{dt} = \frac{L}{T}\frac{\beta'}{\beta_f}\frac{V_p}{V_u}\left(\frac{\partial P}{\partial x}\right)_{x=0} \tag{4}$$

$$-\frac{dP_d}{dt} = \frac{L}{T}\frac{\beta'}{\beta_f}\frac{V_p}{V_d}\left(\frac{\partial P}{\partial x}\right)_{x=L} \tag{5}$$

where V_p = intruded pore volume;
V_u = volume of upstream reservoir;
V_d = volume of downstream reservoir;
β_f = fluid compressibility.

These equations represent mass balances for the penetrating species. They are subject to the initial conditions $P_u(0) = P_1$ and $P_d(0) = P_0$. Expressed in terms of dimensionless variables, Equations (4) and (5) become Equations (6) and (7), respectively.

Table 1
Terms Present in Equation (3).

References	(I)	(II)	(III)	Comment
Brace et al. (1968)	X			quasi-steady
Hsieh et al. (1981)	X		X	---
Pommersheim and Scheetz (1989)	X			quasi-steady
This work	X	X		quasi-steady ($V_u = V_d$)
General solution found	X	X	X	solution has not been

$$-\frac{dp_u}{d\theta} = \frac{\beta'}{\beta_f \varepsilon} \frac{V_p}{V_u} \left(\frac{\partial p}{\partial z}\right)_{z=0} \tag{6}$$

$$-\frac{dp_d}{d\theta} = \frac{\beta'}{\beta_f \varepsilon} \frac{V_p}{V_u} \left(\frac{\partial p}{\partial z}\right)_{z=1} \tag{7}$$

where p_u and p_d are the dimensionless pressures given by $p_u = (P_u - P_0)/\Delta P$ and $p_d = (P_d - P_0)/\Delta P$, respectively. The corresponding dimensionless initial conditions on θ are $p_u(0) = 1$ and $p_d(0) = 0$.

The formulation of Equations (6) and (7) is similar to that of Hsieh et al. (1981). In this development the compressive storage of the reservoirs is taken equal to the fluid compressibility since in practice the reservoirs are generally made from rigid thick-walled metal. This also insures that the boundary conditions do not contain a non-linear term corresponding to the compressibility of the reservoirs themselves.

Equation (3) together with Equations (6) and (7) can be solved numerically to give $p_u(t)$ and $p_d(t)$. This is the general case indicated in Table 1, where a minimum number of simplifying assumptions are made. The numerical solution to this system of equations is not trivial because Equation (3) is a non-linear partial differential equation with time dependent boundary conditions.

As shown in Table 1 the solution presented in this work is a sub-case in which the accumulation of mass [term (III)] within the sample is neglected but the non-linear term (II) is retained. As discussed, the accumulation term can be neglected if observed experimental times are much greater than the characteristic time, i.e., $t >> T$. In this sense T can be considered a system time constant, so that after a number of such periods have passed the system can be considered to have reached almost to steady state and $\partial p/\partial\theta \rightarrow 0$ in Equation (3).*

Model Solution

Since the pressures at the two ends of the sample are continuously changing, pressures within the sample must slowly adjust to accommodate these changes. Under quasi-static conditions, Equation (3) reduces to:

$$\frac{d^2p}{dz^2} + \beta'\Delta P \frac{dp}{dz} = 0 \tag{8}$$

with boundary conditions $p(0) = p_u$ and $p(1) = p_d$.

Equations (4) and (5) are still applicable at quasi-steady state with the partial derivatives being replaced with ordinary derivatives.

An analytical solution to Equations (4), (5) and (6) can be obtained form the important case where the volume of the two reservoirs are equal, i.e., $V_u = V_d$. Details of the solution are provided in Appendix 2. Equations (9), (10) and (11) present expressions for P_u, $P_u - P_d$ and P_f, respectively:

---

* The validity of the quasi-steady state assumption and the application of this criterion to cementitious and other systems is discussed more fully in Part II of this Report.

$$\Phi_u = \frac{P_1 - P_u}{\Delta P} = \frac{1}{(\beta'\Delta P)} \int_0^{t/Tv} [1 - \exp(-Y)]dy \tag{9}$$

where $Y \equiv 2 \tanh^{-1} [e^{-2y} \tanh (\frac{\beta'\Delta P}{2})$

$$\frac{P_u - P_d}{\Delta P} = \frac{Y[t/Tv]}{(\beta'\Delta P)} \tag{10}$$

$$\Phi_f = \frac{P_1 - P_f}{\Delta P} = \frac{1}{(\beta'\Delta P)} \int_0^{\infty} [1 - \exp(-Y)]\, dy \tag{11}$$

where $v = V/V_p$; with V_p = (intruded) pore volume, $V = V_u = V_d$ is the common reservoir volume and Φ_u and Φ_f are reduced pressures.

In implementing the solution, it is convenient to replace the term [1 - exp(Y)] in Equations (9) and (11) by the equivalent form:

$$1 - \exp(-Y) = \sum_{n=1}^{\infty} (-1)^{n+1} \frac{2^n}{n!} \{\tanh^{-1} [e^{-2Y} \tanh (\frac{\beta'\Delta P}{2})]\}^n \tag{12}$$

This series converges rapidly so that only a moderate number of terms of the summation are needed to guarantee convergence. At large values of the reduced compressibility the identity (Jolley, 1961)

$$2 \tanh^{-1} [e^{-2y} \tanh b/2] = \ln [\frac{e^{2y} + \tanh b/2}{e^{2y} - \tanh b/2}] \tag{13}$$

is useful in evaluating the summation. To evaluate the integrals in Equations (9) and (11), a four-point Guass-Quadrature integration scheme with variable step size and internal error detection was used (Lewis). In all cases the summation in Equation (12) was evaluated before the integration was performed.

Discussion of Results of Mathematical Model

Equations (9) through (13) can be used collectively to determine the predicted values of P_u and P_d at any time. It follows from Equation (10) that the upstream and downstream pressures approach one another at long times, reaching a common final pressure P_f. P_f can be found using Equation (11). The final pressure is solely a function of the volume ratio v and the reduced compressibility ($\beta'\Delta P$), while the pressures P_u and P_d also depend on the characteristic time.

Figure 4 presents a plot of the reduced final pressure Φ_f vs. the reduced compressibility $\beta'\Delta P$. At low values of $\beta'\Delta P$, $\Phi_f \rightarrow 1/2$, indicating that $P_f \rightarrow (P_0 + P_1)/2$. This agrees with model predictions of other researchers (Brace et al., 1968, Hsieh et al., 1981, Pommersheim and Scheetz, 1989). As discussed in Appendix 1, this result can also be obtained analytically from a limit analysis on Equation (11). At high values of the reduced compressibility, Φ_f varies reciprocally with it according to the limit form:

$$(\beta'\Delta P)\, \Phi_f \rightarrow \int_0^{\infty} \sum_{n=1}^{\infty} \frac{(-1)^{n+1}}{n!} \ln^n(\coth y)\, dy = k_{po} \tag{14}$$

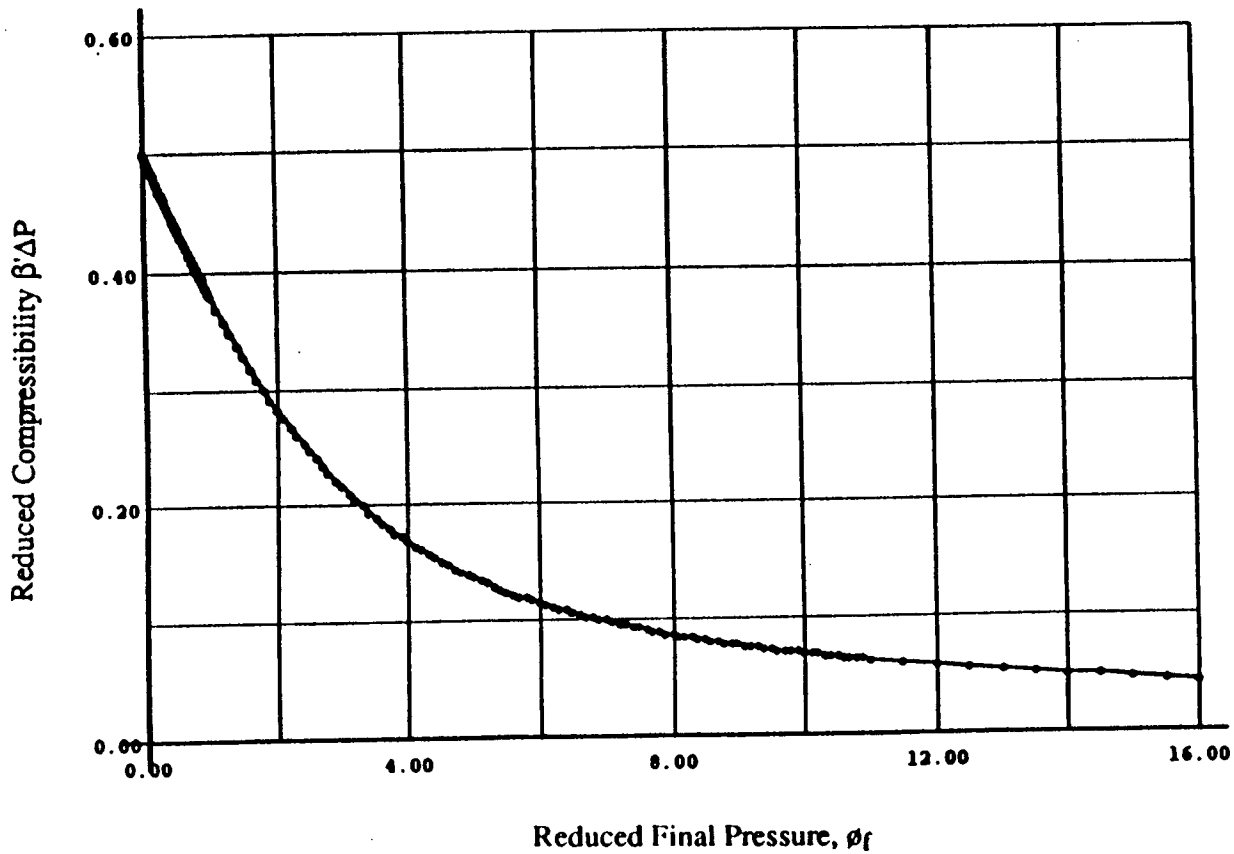

Figure 4. Typical output relating compressibility to reduced final pressure.

Using the integral in Equation (12), the value of the transcendental number k_{po} to five significant figures is 0.69314.

Figure 5 presents a plot of the reduced upstream pressure Φ_u as a function of the reduced time t/Tv, with the reduced compressibility $\beta'\Delta P$ shown as a parameter. For samples of higher compressibility the reduced pressure is less, indicating that the upstream pressure falls less rapidly for such samples. The final pressure reached (dashed asymptote) is greater than for
samples of lower compressibility, which agrees with the results illustrated in Figure 4. The upper curve in Figure 5 shows the result for incompressible samples ($\beta'\Delta P = 0$). This is identical to the solution originally obtained by Brace et al. (1968) and later by other workers, for the case where $V_u = V_d$, that is:

$$\Phi_u|_{\beta'\Delta P=0} = \frac{1}{2}[1 - e^{-2t/Tv}] \qquad (15)$$

As discussed in Appendix 2, Equation (15) can be obtained analytically from Equation (9) using a limit analysis.

Equipment Design

The permeability equipment including the cell was designed and initially constructed in the Materials Research Laboratory. Figure 1 presented earlier represents a schematic drawing of the arrangement of the overall system showing the location of valves, the up-stream and down-stream reservoirs and the permeability cell. In this design, the pressure pulse is applied to the system by rapidly reducing the pressure of the down-stream reservoir. Recovery time from this perturbation is typically on the order of 10 to 15 minutes.

Figure 6 is an exploded diagram of the permeability sample cell showing the physical arrangement of its parts. The current cell uses a thick "Tygon" tube for the sleeving material. This material has been found to be superior to rubber sleeving in that it does not readily puncture under the influence of confining pressure in the presence of surface imperfections in the sample. Three cell sizes are available which can accommodate samples of 1", 2" and 3" in diameter and lengths varying up to 6". Figure 7 is a detailed engineering drawing of the assembled cell.

The pressure response of the experiment is monitored electrically with SCHAEVITZ piezoelectric transducers designed to operate over a pressure range from 0 to 1000 psi. The emf output of the transducers is monitored on an IBM PC computer into which a METRABYTE DAS-8 data acquisition and control board was installed.

The computer control of the data acquisition is achieved with a compiled DOS algorithm. The program reads the analog inputs to a file for storage which can be annotated with a descriptive text file for archiving purposes. Data acquisition time is selected by the operator. The output file of this program is stored separately on a 5.25" floppy disc and further processing is accomplished by reading this raw data into another routine called "convert" which transforms the raw data into a psi vs. time file which can be read into LOTUS 123 for final data processing.

Sample Handling

In order for this apparatus to work, all specimens to be tested must be fully water saturated before the experiment is initiated. Water saturation is achieved by vacuum

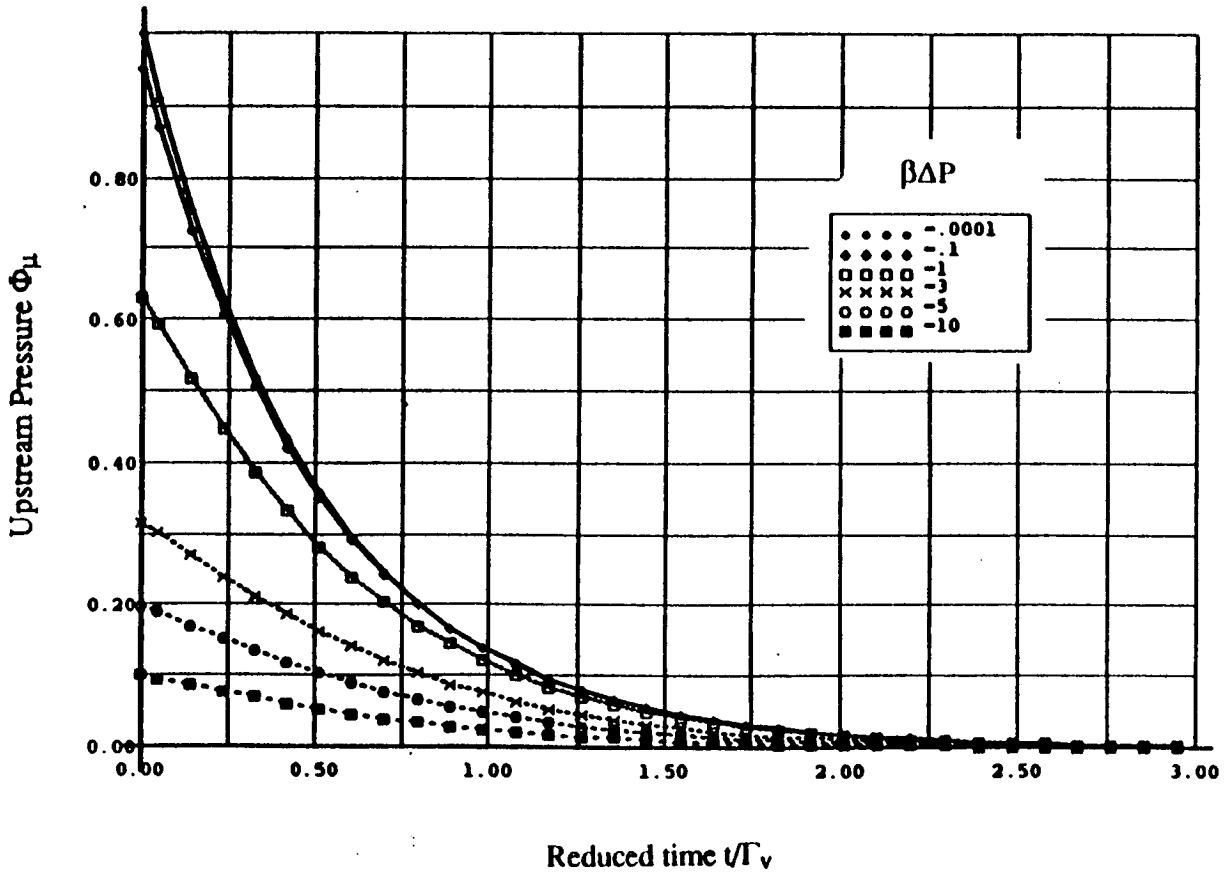

Figure 5. Typical output of upstream pressure and reduced time for varying βΔP.

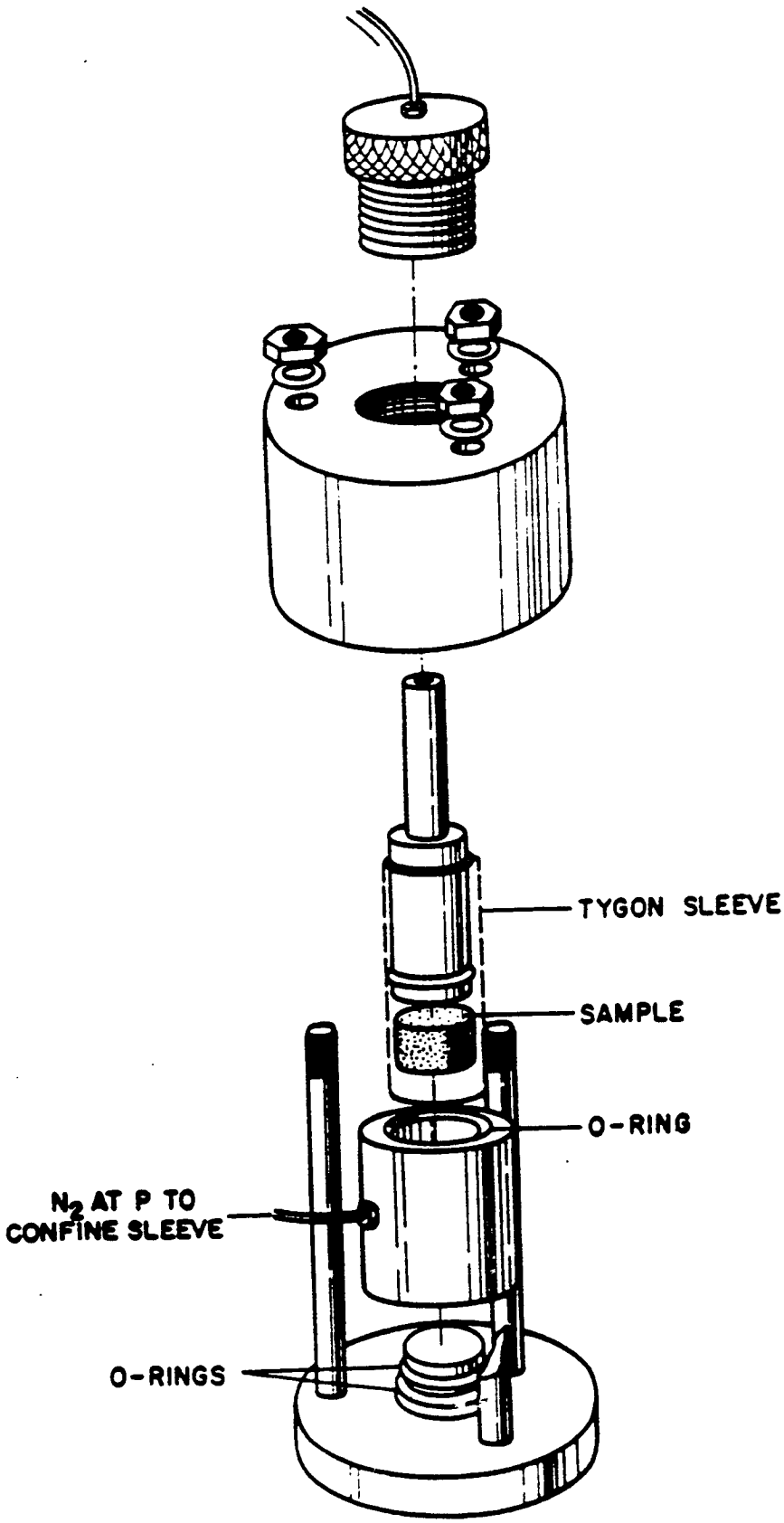

Figure 6. Exploded diagram of permeability cell.

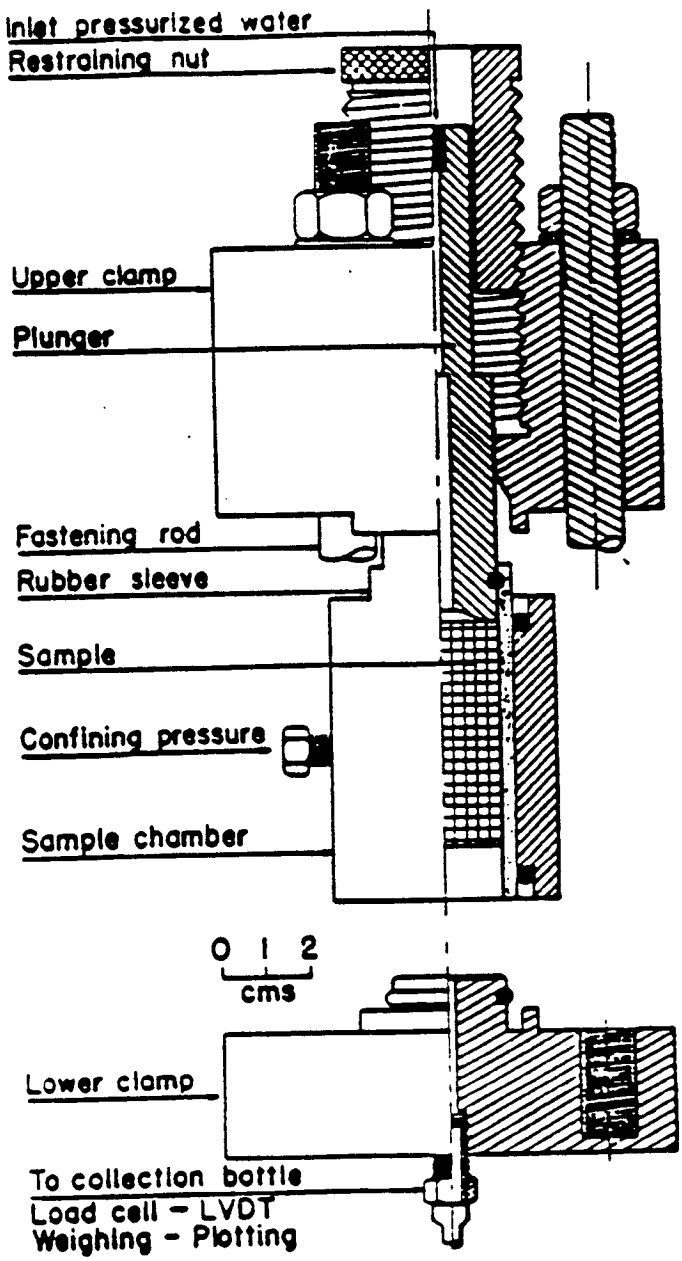

Figure 7. Sectional view of the liquid permeability apparatus.

impregnation; the sample is placed in the vacuum produced by a roughing pump for 24 hours before it is immersed in deionized water. The water saturated specimen is then placed in the sleeving material and the cell assembled according to the detailed procedure which appears in the SHRP 201 Fourth Quarterly Report (1989).

Typical Experimental Results

Measurements have been made on several samples of the Tuscarora sandstone, actually an orthoquartzite, for calibration purposes. The initial theory adequately describes the pressure decay characteristics and permeability. Figures 8a,b are examples of the output of the apparatus. Figure 8a represents the pressure readings for the upper- and lower-transducers recorded for the course of an experimental lasting approximately 1200 minutes. When these data are processed as described above, a straight line, as shown in Figure 8b, is produced.

Initial data collection for cement pastes and mortars has been inconsistent with the mathematical theory upon which the experiment was designed. A considerable amount of time has been expended in order to reconcile the differences between the observed "extended" exponential decay of these materials. The results of these experiments will require that additional modifications to the theory be made in order to adequately interpret the observed pressure decay.

Measurements on several samples of the quartzite have resulted in a permeability of 9×10^{-8} darcys. This value is consistent with previous permeability measurements measured using both liquid (water) and gas systems: 1.7×10^{-7} and 3.6×10^{-7} darcys respectively. The slightly lower value is attributed to differences in the confining pressures between the two experiments. These comparisons strongly suggest that the apparatus is functioning properly. Further, the nature of the data collected for sandstone clearly show, at least for this kind of material, that the mathematical analysis developed is valid.

A comparison of Panel A in Figures 8 and 9 reveal the same general form of the decay/pressure rise transducers curves. The processed data for a cement paste are presented in Figure 9, Panel B. The "extended" exponential form for the data differs from that of the rock (Figure 8) and will require modification to the mathematical model.

Limitation of the Equipment

The apparatus has been designed to measure very low fluid flow, below the range of a nanodarcy. This permeability region is of particular interest because many of our previous samples of concrete and mortars had very low flow rates. As described earlier, the apparatus designed has been successful, however, we have seen that in order to obtain representative data describing the flow of fluid through a concrete specimen, the pressure **must** be equilibrated throughout the interior of the specimen. Equilibration of the pressure is monitored by establishing a reverse flow through the test sample. That is, P_u is placed at a lower pressure than P_d and then reversed before the test data is formally collected. Herein lies the crux of the problem. The time required to reach this equilibrium is of the same order of magnitude as that required to conduct the experiment (Roy, 1988), which could be several seconds to minutes for specimens with flow greater than a microdarcy or from days to weeks or longer for sub-nanodarcy specimens. Figure 10 represents the times required to saturate test specimens. The data in this figure are characteristic only of one set of conditions in which the sample is assumed to be one inch in diameter and one inch in length with a totally dry porosity of 25%. The principal data were determined by solving darcy's law for the volume of water necessary to fill the 25% porosity at varying permeabilities and a fixed pressure differential. As can be seen, times to saturation can be

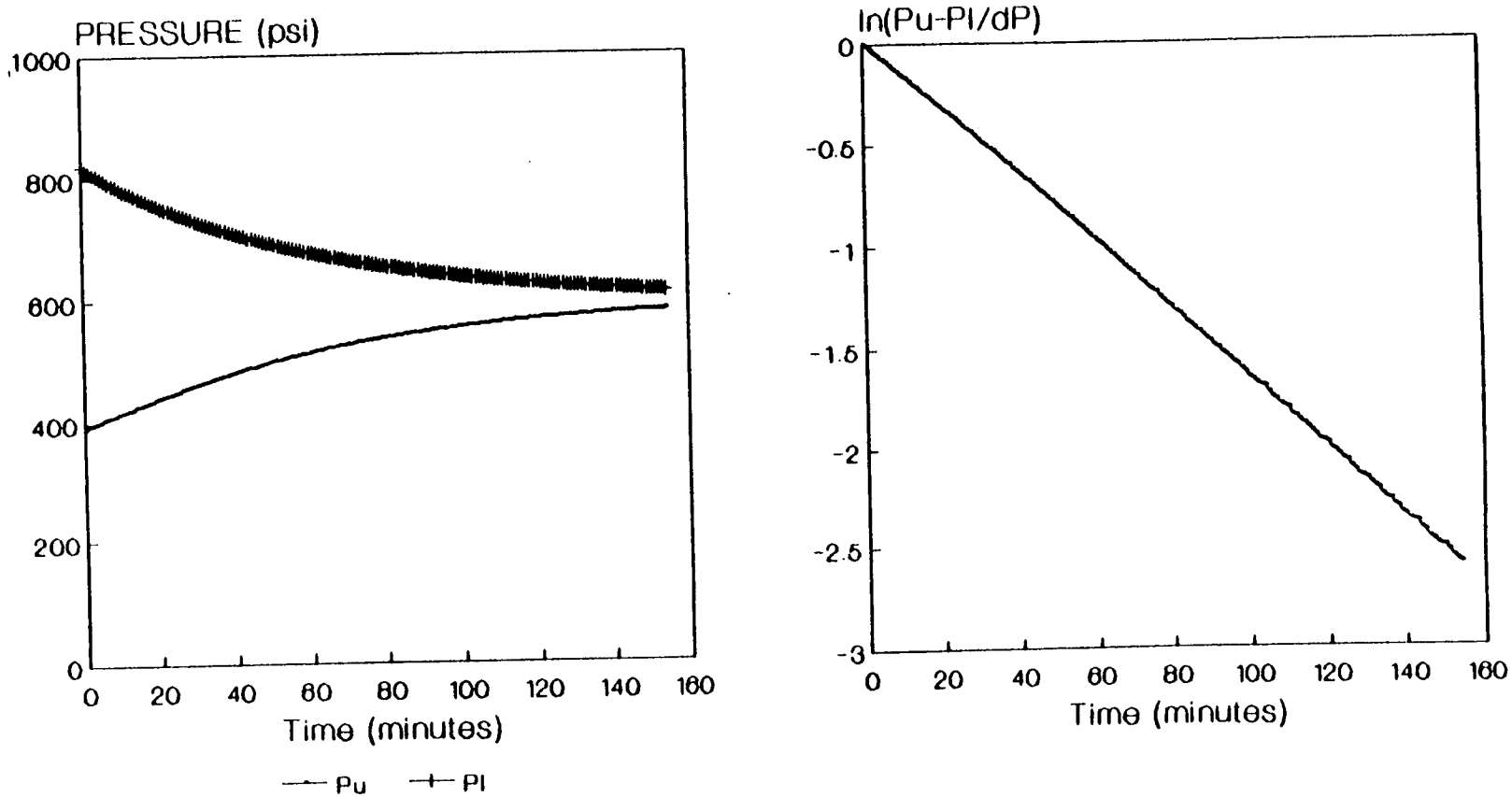

Figure 8. (A) Raw data [pressure (psi)] for Tuscarora quartzite. (B) Processed data fromwhich permeability is calculated.

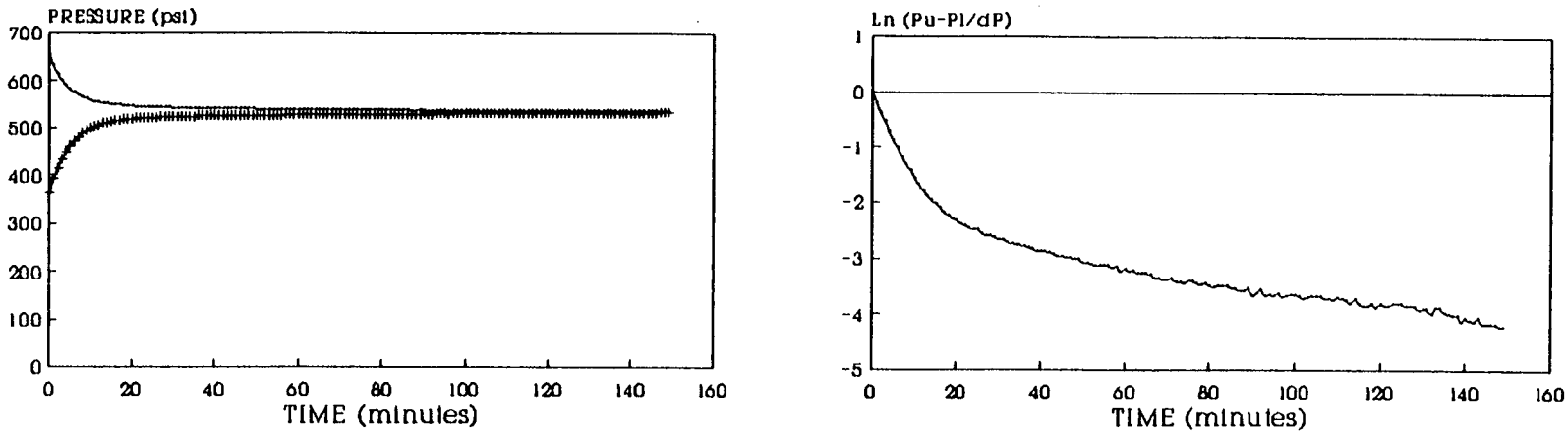

Figure 9. (A) Raw data for cement paste shows pressure decay and rise curves. (B) Processed data showing "extended" exponential-like behavior.

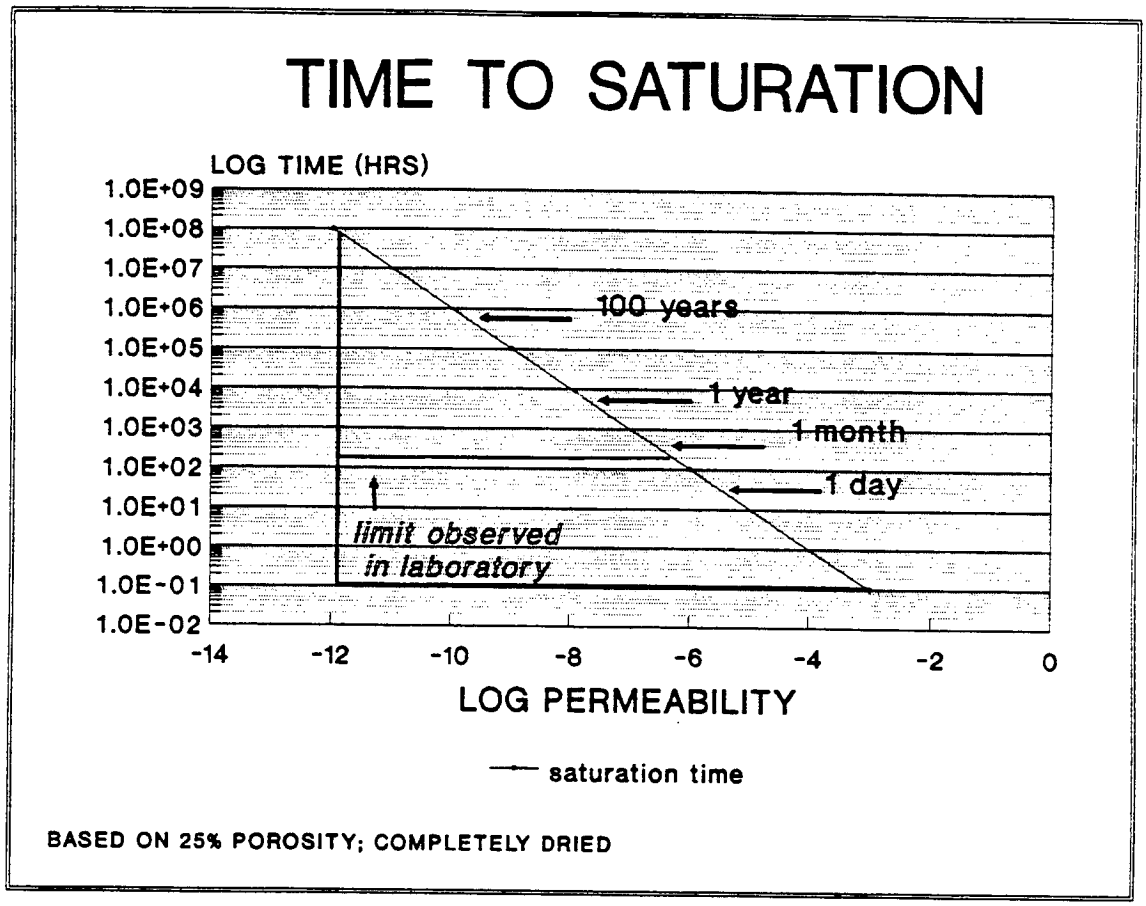

Figure 10. Bounding calculation of the time necessary to saturate a completely dried test specimen with 25% porosity. All calculations are based upon solving darcy's equation at fixed permeabilities for the time necessary to fill the porosity at a fixed pressure. The parameters used in this calculation are necessarily the same as the test equipment design.

very long. The horizontal line segment represents the practical limit of laboratory usage from this research. Attempts to enhance pressure equilibration by using elevated hydrostatic pressure before conducting the data collection will only very slightly assist in reducing the time required to equilibrate the sample.

In an open porous system where only capillary action is responsible for backfilling the porosity, the following relation controls the fraction of the capillary volume filled:

$$X = 1/[1 + (rP'/2Y\cos\theta)]$$

where:
- X = fraction capillary volume filled
- r = critical pore radius
- Y = surface tension of water
- θ = contact angle
- ρ' = pressure.

This relationship suggests that at atmospheric pressure only 91% of the volume of a single capillary 150 nm in radius will be filled with water under capillary action. If the pressure is raised to 700 psi, only 95% of the single capillary will be filled. For interest in this permeability application, the rate at which this capillary will fill is known as Poiseuille's Law:

$$L^2 = [Y\cos\theta/2n]rt$$

where:
- L = penetration length
- t = time
- Y = surface tension of water
- θ = contact angle
- r = critical pore radius
- n = viscosity of water.

To completely penetrate the single capillary 150 nm in radius, according to this relationship, would take on the average 37 years.

Although these calculations represent only bounding approximation, they suggest that very low values of permeability can only be achieved at the expense of lengthy sample pretreatment.

References

W.F. Brace, J.B. Walsh and W.J. Frangos, "Permeability of Granite Under High Pressure," J. Geophys. Res. 73 (6), 2225-2236 (1968).

J.D. Hooton and J.D. Wakeley, "Influence of Test Conditions on the Water Permeability of Concrete in a Triaxial Cell," Materials Research Society Symposium P, 1988, MRS Press, Pittsburgh, PA (in press).

P.A. Hsieh, J.V. Tracy, C.E. Neuzil, J.D. Bredehoeft and S.E. Silliman, "A Transient Laboratory Method for Determining the Hydraulic Properties of 'Tight' Rocks — I. Theory," Int. J. Rock Mech. Min. Sci. & Geomech. Abstr. 18, 245-252 (1981).

L.B.W. Jolley, Summation of Series, 2nd Revised Ed., Dover Publications, New York (1961).

W. Lin, "Compressible Fluid Flow Through Rocks of Variable Permeability," Report UCRL-52304, Lawrence Livermore Laboratory, University of California, Livermore (1977).

C.E. Neuzil, C. Cooley, S.E. Silliman, J.D. Bredehoeft and P.A. Hsieh, "A Transient Laboratory Method for Determining the Hydraulic Properties of 'Tight' Rocks — II. Application, Int. J. Rock Mech. Min. Sci. & Geomech. Abstr. 18, 253-258 (1981).

J. Pommersheim and B. Scheetz, "Extension of Standard Methods for Measuring Permeabilities by Pressure Pulse Testing," to be submitted for publication (1989).

D.M. Roy, "Relationships Between Permeability, Porosity, Diffusion and Microstructure of Cement Pastes, Mortar and Concrete at Different Temperatures," Materials Research Society Symposium P, 1988, MRS Press, Pittsburgh, PA (in press).

D. Trimmer, "Design Criteria for Laboratory Measurements of Low Permeability Rocks," Geophys. Res. Lett. 8 (9), 973-975 (1981).

SHRP 201, Fourth Quarterly Report (1989).

APPENDIX 1: Derivation of Equation (1)

This appendix presents a derivation of the conservation equation for flow of a compressible liquid in a porous medium, expressed solely in terms of pressure.

The mass conservation or continuity equation for the liquid is:

$$\varepsilon \frac{\partial \rho}{\partial t} = \nabla \cdot \rho \vec{v} \qquad \text{(A-1)}$$

where ρ is the liquid density and v is the superficial local fluid velocity, based on the overall cross-section. The constitutive rate equation for flow in porous media is Darcy's equation:

$$\vec{v} = -\frac{k}{\mu} \nabla P \quad . \qquad \text{(A-2)}$$

Substituting Equation (A-2) into (A-1):

$$\frac{\partial \rho}{\partial t} = \frac{k}{\varepsilon \mu} \nabla \cdot \rho \nabla P \quad . \qquad \text{(A-3)}$$

Inthe above equations, the dependent variables $\vec{v}$, P and ρ are considered to be mean quantities, averaged over a section of flow large when compared to mean pore sizes.

From the phase rule $\rho = f(T,p)$, it follows that:

$$\frac{d\rho}{\rho} = \beta_T dP - \beta_p dT \qquad \text{(A-4)}$$

where β_p, the volume expansivity, is given by $-\frac{1}{\rho}\left(\frac{\partial \rho}{\partial T}\right)_p$,

and β_T, the isothermal compressibility, is $\frac{1}{\rho}\left(\frac{\partial \rho}{\partial p}\right)_T$.

At constant temperature, Equation (A-5) can be integrated to give:

$$\rho = \rho_p e^{\beta_T P} \qquad \text{(A-5)}$$

where ρ_p is the density at low pressure. In the derivation of Equation (A-6) it is presumed that the isothermal compressibility does not vary significantly with pressure over the pressure range employed.

Equation (A-5) can be considered to be the equation of state for the liquid, describing how its density changes with pressure. Substituting it into Equation (A-3):

$$\varepsilon \frac{\partial \rho}{\partial t} = \frac{k}{\mu} \nabla^2 \rho = \frac{k}{\mu} \frac{\partial^2 \rho}{\partial x^2} \quad . \qquad \text{(A-6)}$$

Here the assumption if made of one dimensional flow (in the x direction) with constant transport area.

The pressure form of Equation (A-6) can be obtained by substituting the equation of state (A-5), when:

$$\frac{\partial^2 P}{\partial x^2} + \beta_T \left(\frac{\partial P}{\partial x}\right)^2 = \frac{\beta_T \mu}{k} \frac{\partial P}{\partial t} \qquad \text{(A-7)}$$

Equation (A-7) is the same as Equation (1) of the text, with β_T taken equal to β', the sample compressibility.

APPENDIX 2: Solution of Equation (8)

This appendix provides details to the analytical solution of Equation (8) as given by Equations (9), (10) and (11). Equations (6) and (7) are also involved since they represent boundary conditions on Equation (8). The solution predicts reservoir pressures as a function of time.

Making the transformation, $q = dp/dz$, Equation (8) becomes:

$$q \frac{dq}{dp} + \beta' \Delta P \, q^2 = 0 \quad . \tag{A-8}$$

At quasi-steady state, this equation is subject to the boundary conditions $p(0) = p_u$ and $p(1) = p_d$. Separating variables and integrating twice to recover p:

$$\frac{p - p_d}{p_u - p_d} = \frac{1}{\beta' \Delta P} \ln \left[e^{\beta' \Delta P} + z(1 - e^{\beta' \Delta P}) \right] \quad . \tag{A-9}$$

At low values of $\beta' \Delta P$ Equation (A-9) can be shown to reduce to:

$$\frac{p - p_d}{p_u - p_d} = 1 - z \quad . \tag{A-10}$$

Equation (A-10) predicts a linear pressure gradient across the sample. It is equivalent to the result obtained by Brace et al. (1968).

Application of Equations (6) and (7), to Equation (A-9) yields Equation (A-12) and (A-13), respectively:

$$- \frac{\beta_f \varepsilon V_u}{\beta' V_p} \frac{dp_u}{d\theta} = 1 - \exp \left[-\beta' \Delta P (p_u - p_d) \right] \quad , \tag{A-11}$$

$$\frac{\beta_f \varepsilon V_d}{\beta' V_p} \frac{dp_d}{d\theta} = \exp \left[-\beta' \Delta P (p_u - p_d) \right] - 1 \quad . \tag{A-12}$$

For the case when reservoir volumes are equal ($V_u = V_d = V$) adding Equations (A-12) and (A-13) gives:

$$\frac{du}{d\theta} = \frac{\beta' V_p}{\beta_f \varepsilon V} \left\{ \exp \left[-(\beta' \Delta P) u \right] - \exp \left[(\beta' \Delta P) u \right] \right\} \tag{A-13}$$

u, the new dependent variable, is equal to $P_u - P_d$. Separating variables and integrating with the initial conditions $u(0) = 0$, and expressing the result in terms of the original variables:

$$\tanh \left[\frac{(P_u - P_d)\beta'}{2} \right] = \exp \left(-\frac{2t}{T_v} \right) \cdot \tanh \left(\frac{\beta' \Delta P}{2} \right) \quad . \tag{A-14}$$

Equation (A-15) can be rearranged to given Equation (8) of the text. In the limit, as $(\beta' \Delta P) \rightarrow 0$, it can be shown using Equation (11) that Equation (A-15) reduces to the solution found by Pommersheim and Scheetz (1989):

$$\ln\left[\frac{P_u - P_d}{\Delta p}\right] = -\frac{2t}{Tv} \quad . \tag{A-15}$$

The other equations of the text can be derived in a similar manner. Thus Equation (7) is obtained by substituting Equation (8) into Equation (A-12), separating variables and integrating, while Equation (9) is simply the long time form of Eqation (7). Equation (13) results from Equation (7) by letting $\beta'\Delta P \rightarrow 0$.